

Supporting Information

Hollow spheres consisting of $\text{Ti}_{0.91}\text{O}_2/\text{CdS}$ nanohybrids for CO_2 photofixation

Wenguang Tu,^{a, b, c} Yong Zhou,^{*, a, b, c} Shichao Feng,^{a, b, c} Qinfeng Xu,^{b, d} Peng Li,^e
Xiaoyong Wang,^b Min Xiao,^b and Zhigang Zou^{*, b, c}

^{a.} Key Laboratory of Modern Acoustics, MOE, Institute of Acoustics, School of Physics, Nanjing University, Nanjing 210093, P. R. China; E-mail: zhouyong1999@nju.edu.cn

^{b.} National Laboratory of Solid State Microstructures, Department of Physics, and Collaborative Innovation Center of Advanced Microstructures, Nanjing University, Nanjing 210093, China; E-mail: zgrou@nju.edu.cn

^{c.} Ecomaterials and Renewable Energy Research Center (ERERC), Nanjing University, Nanjing 210093, China

^{d.} Department of Physics and Optoelectronic Engineering, Ludong University, Yantai 264025, P. R. China

^{e.} Environmental Remediation Materials Unit and International Center for Materials Nanoarchitectonics (WPI-MANA), 1-1 Namiki, Tsukuba, Ibaraki 305-0044, Japan.

E-mail: zhouyong1999@nju.edu.cn; zgrou@nju.edu.cn

Methods

Materials. Poly(methyl methacrylate) (PMMA) sphere was of an average diameter of 0.3 μm . Polyethylenimine (PEI), a cationic polyelectrolyte, was purchased from Alfa Aesar and used as received. $\text{Ti}_{0.91}\text{O}_2$ nanosheets were prepared using Sasaki's method.¹ The water-soluble CdS NPs were synthesized by a previous reported method.² Distilled water was used in all experiments.

Preparation of ultrathin multilayer hollow spheres consisting of alternating

Ti_{0.91}O₂ nanosheets and CdS NPs. The detailed synthetic procedure of ultrathin multilayer hollow spheres consisting of alternating Ti_{0.91}O₂ nanosheets and CdS NPs via combination of the LBL assembly technique and a microwave is outlined below. 1 g of PMMA spheres were dispersed in 200 ml of H₂O containing 0.5 g of PEI at pH 9.0 under stirring. Dilute HCl or ammonia solutions were used to adjust the pH. The solution was ultrasonically treated for 10 min and then stirred for 15 min to ensure the saturated adsorption of PEI on PMMA surfaces. Excess PEI was removed by twice centrifugation and wash cycles. Then, the PEI-coated PMMA was dispersed in 200 ml of H₂O at pH 9.0 with ultrasonic treatment for 10 min. A portion of colloidal suspension of negatively charged Ti_{0.91}O₂ nanosheets at pH 9.0 was added to the turbid PMMA suspension under stirring until supernatant was almost transparent and the resulting product was sedimented, owing to the electrostatic interaction of the oppositely charged nanosheets and PMMA surface. Resulting material was recovered by the separation and washing process, and excess Ti_{0.91}O₂ nanosheets were removed simultaneously. The above procedure was repeated until 5 bilayers of (PEI/Ti_{0.91}O₂/PEI/CdS)₅ have been deposited onto PMMA spheres. Finally, the resulting product was dispersed in water by sonication and dried by lyophilization. 0.1 g of dried sample in carbon powder-surrounding crucible was placed inside a conventional microwave oven in argon (Ar) atmosphere. The microwave oven (Galanz G80F20CN1L-DG (SO)) was operated at full power (800 W), 2.45 GHz, in 200 s cycles (on for 150 s, off for 50 s) for a total reaction time of 600s. During microwave irradiation, PEI moiety was removed and PMMA particles were

decomposed. After reaction, hollow spheres consisting of alternating $\text{Ti}_{0.91}\text{O}_2$ nanosheets and CdS QDs were obtained, and trifling PMMA residue was removed with tetrahydrofuran (THF). The hollow spheres with $(\text{Ti}_{0.91}\text{O}_2)_5$ shell or with $(\text{CdS NPs})_5$ shell were obtained by the analogous procedure for comparison.

Characterization. The morphology of the samples was observed by scanning electron microscopy (SEM, FEI NOVA NanoSEM230, USA) and transmission electron microscopy (TEM, JEOL 3010, Japan). The UV-visible (UV-vis) diffuse reflectance spectra were recorded with a UV-vis spectrophotometer (UV-2550, Shimadzu) at room temperature and transformed to the absorption spectra according to the Kubelka–Munk relationship. The samples were analyzed with X-ray photoelectron spectroscopy (XPS) (K-Alpha, THERMO FISHERSCIENTIFIC). The XPS spectrum was calibrated with respect to the binding energy of the adventitious C1s peak at 284.8 eV.

PL spectral measurements and transient time-resolved PL decay measurements.

The 800 nm output of a 76 MHz, picosecond Ti:Sapphire laser was used to get the wavelengths of 266 nm from the second and third harmonic generation processes, respectively. For PL spectral measurements, 266 nm beam with a power density of $\sim 100\text{W}/\text{cm}^2$ was focused onto the sample surface at an incident angle of $\sim 45^\circ$ relative to the normal direction. The sample PL was collected vertically from the surface by a microscope objective and sent through a 0.5 m spectrometer to a charge-

coupled-device camera. For transient time-resolved PL decay measurements, 266 nm laser beam was focused on the sample surface by a microscope objective also at a power density of ~ 100 W/cm². The sample PL was collected by the same objective and sent to an avalanche photodiode in the time-correlated single-photon counting system with a time resolution of ~ 250 ps. All the measurements were performed at room temperature.

Photocatalytic experiments. In the photocatalytic reduction of CO₂, the 0.01g of sample was uniformly dispersed on the glass reactor with an area of 4.2 cm². A 300W Xenon arc lamp was used as the light source of photocatalytic reaction. The volume of reaction system was about 230 ml. The reaction setup was vacuum-treated several times, and then the high purity of CO₂ gas was followed into the reaction setup for reaching ambient pressure. 0.4 mL of deionized water was injected into the reaction system as reducer. The as-prepared photocatalysts were allowed to equilibrate in the CO₂/H₂O atmosphere for several hours to ensure that the adsorption of gas molecules was complete. During the irradiation, about 0.5 mL of gas was continually taken from the reaction cell at given time intervals for subsequent CH₄ concentration analysis by using a gas chromatograph (GC-2014B, Shimadzu Corp., Japan). All samples were treated at 350 °C for 1 h at vacuum for removal of organic adsorbates before the photocatalysis reaction.

Data analysis. The normalized fluorescence decay traces of hollow spheres with

(Ti_{0.91}O₂)₅ and (CdS QDs)₅ shells is perfectly fitted to a single exponential function in the form of $f(t) = \exp(-t/\tau)$. The decay behavior of Ti_{0.91}O₂/CdS hollow spheres is not well-fitted by a single exponential function, but it can be well-fitted to a biexponential function in the form of $f(t) = A_1 \exp(-t/\tau_1) + A_2 \exp(-t/\tau_2)$. The average lifetime τ is calculated by the expression in the form of $\tau = (A_1 \tau_1^2 + A_2 \tau_2^2)/(A_1 \tau_1 + A_2 \tau_2)$.

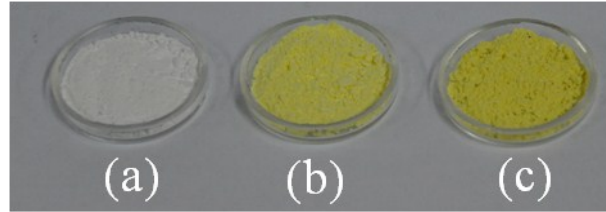


Fig. S1 Photographs of PMMA spheres coated with (a) $(\text{PEI}/\text{Ti}_{0.91}\text{O}_2)_5$, (b) $(\text{PEI}/\text{CdS})_5$ and (c) $(\text{PEI}/\text{Ti}_{0.91}\text{O}_2/\text{PEI}/\text{CdS})_5$ shells.

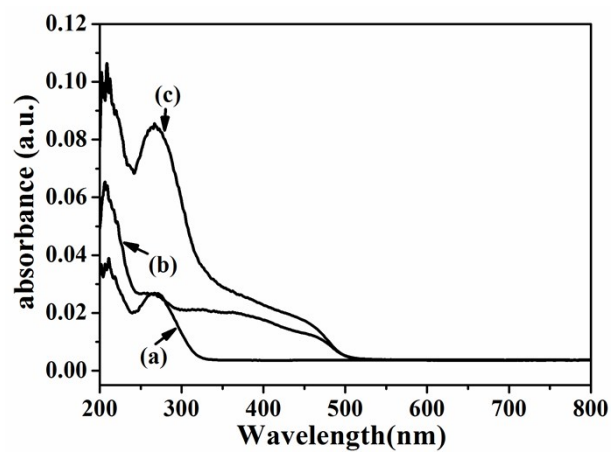


Fig. S2 UV-vis diffuse reflectance spectra of PMMA spheres coated with (a) $(\text{PEI}/\text{Ti}_{0.91}\text{O}_2)_5$, (b) $(\text{PEI}/\text{CdS})_5$ and (3) $(\text{PEI}/\text{Ti}_{0.91}\text{O}_2/\text{PEI}/\text{CdS})_5$ shells.

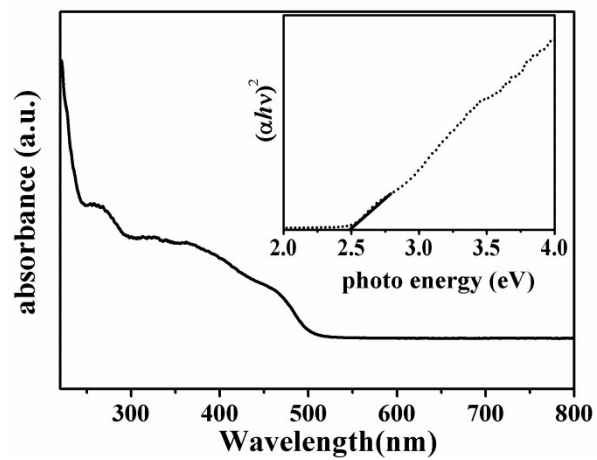


Fig. S3 UV-vis diffuse reflectance spectra of PMMA spheres coated with (PEI/CdS)₅.

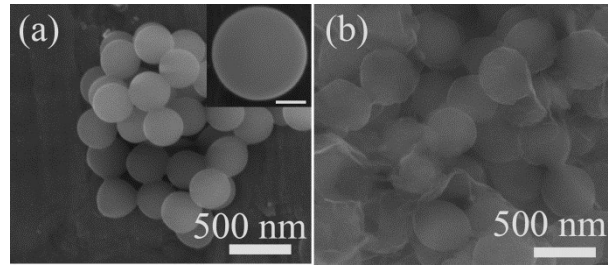


Fig. S4 SEM images of (a) bare PMMA spheres, (b) PMMA spheres coated with (PEI/Ti_{0.9}O₂/PEI/CdS)₅. The scale bare of the inset (a) is 100 nm.

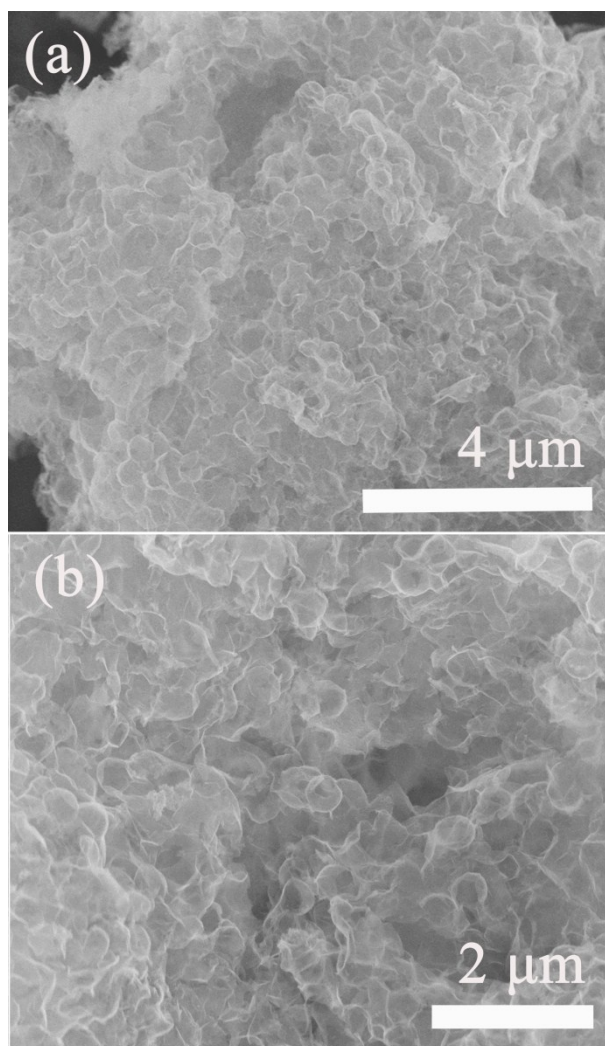


Fig. S5 FE-SEM images of $\text{Ti}_{0.91}\text{O}_2/\text{CdS}$ hollow spheres.

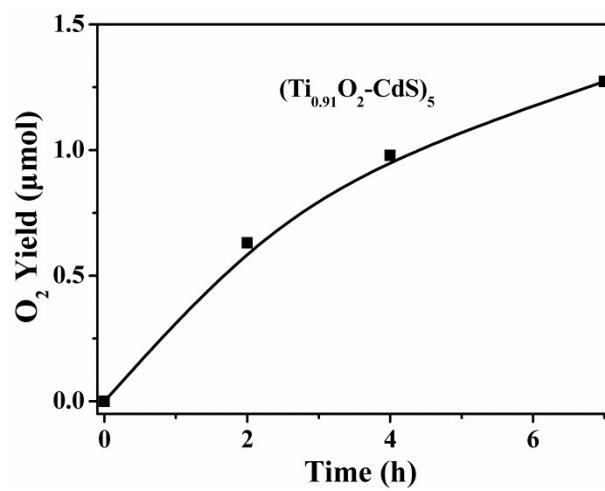


Fig. S6 Photocatalytic O₂ evolution amounts over (Ti_{0.91}O₂/CdS)₅ hollow spheres shells. Samples: 0.01 g

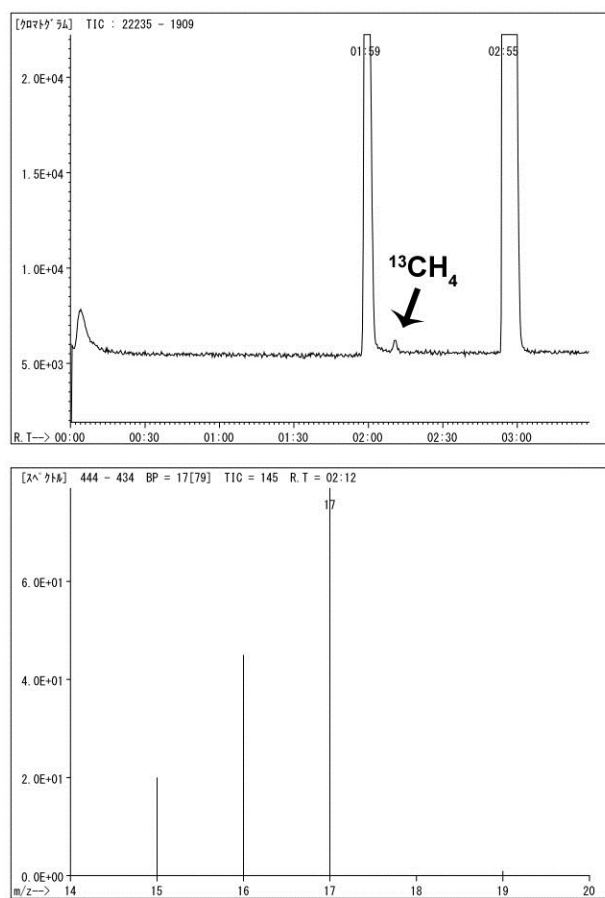


Fig. S7 Gas chromatogram (top) and mass spectrum of $^{13}\text{CH}_4$ (down). Carbon dioxide $^{13}\text{CO}_2$ was used.

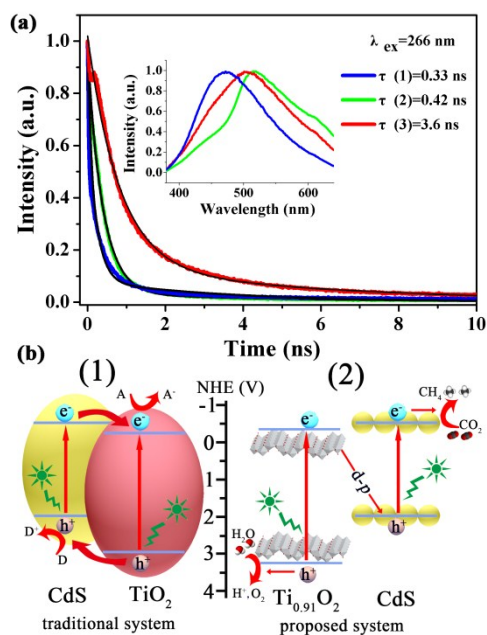


Fig. S8 (a) PL decay traces of Ti_{0.91}O₂ hollow spheres (blue), CdS hollow spheres (green) and Ti_{0.91}O₂/CdS hollow spheres (red). The inset is the PL emission spectra of Ti_{0.91}O₂ hollow spheres (blue) and Ti_{0.91}O₂/CdS hollow spheres (red). (b) Schematic illustration of traditional TiO₂-CdS system (route 1) and artificial Z-scheme system (route 2).

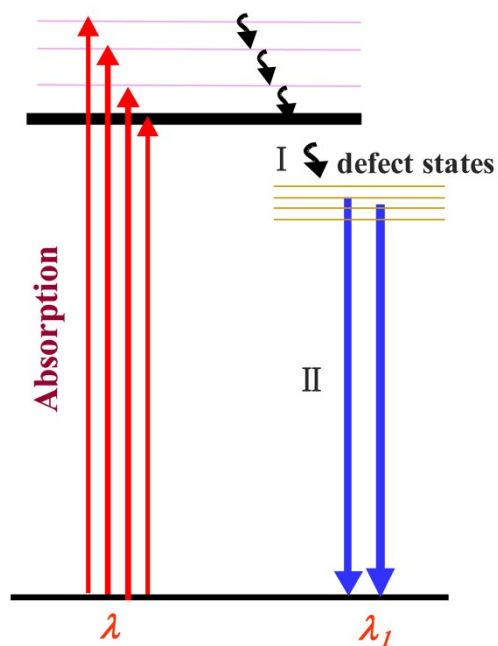


Fig. S9 A schematic illustration of PL mechanism from CdS NPs. ‘I’ refers to non-radiative transition process, and ‘II’ refers to radiative transition process.

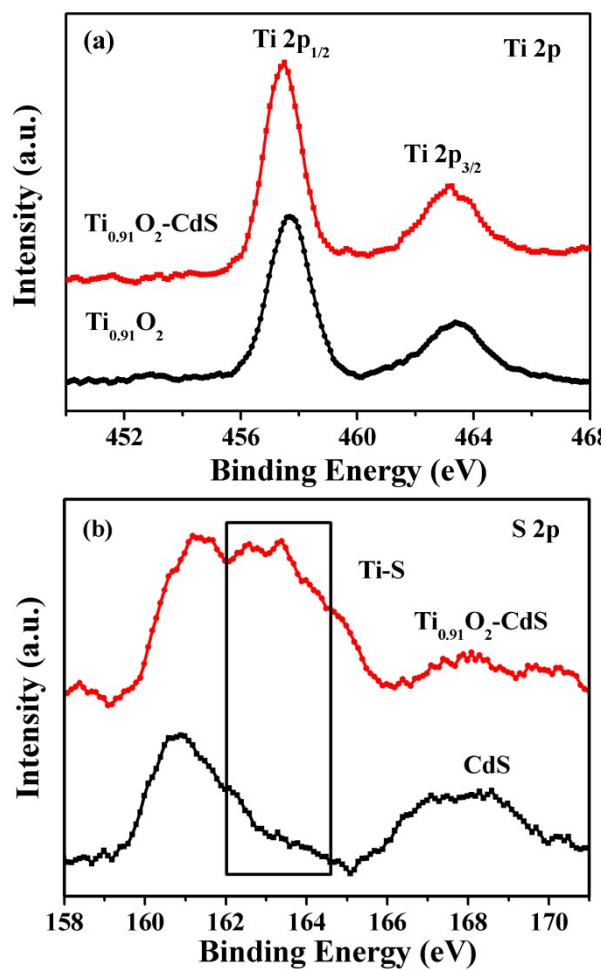


Fig. S10 Ti 2p and S 2p XPS spectra of CdS, Ti_{0.91}O₂, and Ti_{0.91}O₂/CdS hollow spheres.

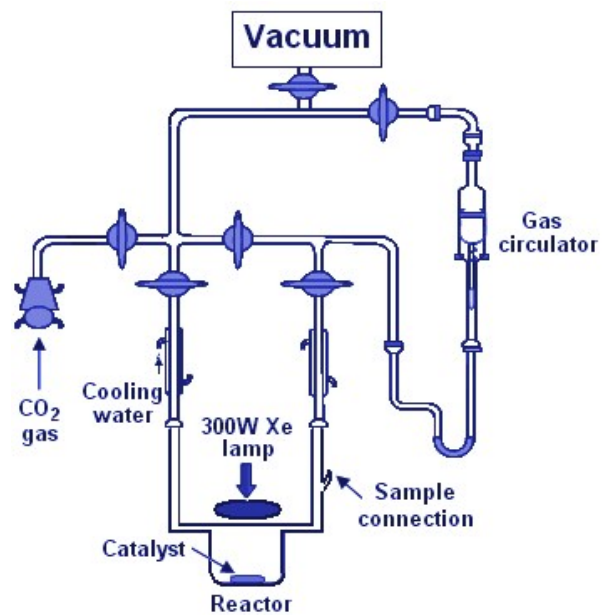


Fig. S11. Reaction setup for evaluation of conversion rate of CO₂.

Table S1. Potocatalytic reduction of CO₂ into CH₄ under Various Conditions.^a

photocatalyst	CO ₂ , UV-vis ($\mu\text{mol h}^{-1}$)	CO ₂ , $\lambda > 420$ nm	Ar, UV-vis
CdS	×	×	×
Ti _{0.91} O ₂	0.014 ^b	×	×
Ti _{0.91} O ₂ /CdS	0.1 ^b	×	×
P25	0.069 ^b	×	×

^a0.01g of photocatalyst. Potocatalytic reaction conditions: CO₂ or Ar gas was followed into the reaction setup for reaching ambient pressure before irradiation using A 300W Xenon arc lamp or with a cutoff filter ($\lambda > 420$ nm). Symbol ‘×’ refers to that photocatalyst shows no performance.

- 1 T. Sasaki and M. Watanabe, *J. Am. Chem. Soc.*, 1998, **120**, 4682; L. Wang, T. Sasaki, Y. Ebina, K. Kurashima and M. Watanabe, *Chem. Mater.*, 2002, **14**, 4827.
- 2 C. Barglik-Chory, D. Buchold, M. Schmitt, W. Kiefer, C. Heske, C. Kumpf, O. Fuchs, L. Weinhardt, A. Stahl, E. Umbach, M. Lentze, J. Geurts and G. Muller, *Chem. Phys. Lett.*, 2003, **379**, 443.